Carbohydrate Polymers 92 (2013) 1133–1142

Contents lists available at SciVerse ScienceDirect

Carbohydrate Polymers

journal homepage: www.elsevier.com/locate/carbpol

Characterisation of commercial LM-pectin in aqueous solution

Xiangyang Li[a], Saphwan Al-Assaf[a,*], Yapeng Fang[a], Glyn O. Phillips[a,b]

[a] Glyn O Phillips Hydrocolloids Research Centre, Glyndwr University, Wrexham LL11 2AW, UK
[b] Phillips Hydrocolloid Research Ltd., 45 Old Bond Street, London W1S 4AQ, UK

ARTICLE INFO

Article history:
Received 5 March 2012
Received in revised form
24 September 2012
Accepted 28 September 2012
Available online 13 October 2012

Keywords:
Aggregation/association
LM-pectin
Intrinsic viscosity
Rheology
Dynamic light scattering
Hydrogen bonding induced aggregation
Ca-induced aggregation

ABSTRACT

Fourteen commercial LM-pectin samples were investigated in this study. The degree of esterification (DE) varied from 9.6% to 42.0% and the degree of amidation (DA) from 0% to 25%. Chemical and structural characteristics were examined using atomic absorption (AA), dilute solution capillary viscometry, GPC-MALLS and dynamic light scattering. The intrinsic calcium was in the range of 47–1388 ppm, the intrinsic viscosity varied from 2.9 to 4.9 (dL/g) and the weight average molecular weight (M_w) from 113 to 290 (kDa). Most of the samples had Huggins constants of ~0.5. However, for samples having acidic pH, Huggins constant values greater than 1, which can be as an indication of aggregation, were obtained. The high Huggins constant value could be reduced to ~0.5 by the addition of 3 M urea, indicating that the aggregation was stabilised by hydrogen bonding. Shear flow viscosity revealed three types of rheological behaviour. Type A showed pronounced shear thinning behaviour, which was reduced by the addition of hydrogen bonding breaking agent urea. Type B with intrinsic Ca of 1 mM and pH ~4 showed two shear thinning regions, with significantly enhanced shear viscosity upon addition of calcium. Type C showed the least aggregation due to its pH ~4 and low intrinsic Ca, but could be converted to type B upon addition of Ca. The effect of Ca on the rheological behaviour of types B and C was further confirmed by $CaCl_2$ and Ca-chelating agent (EDTA). Temperature affected the molecular conformation of all types and most significantly type A by eliminating the hydrogen bonding.

1. Introduction

Pectin is an anionic biopolymer widely used in food, pharmaceutical and technical applications due to its structural diversity. Commercial pectin is mainly extracted from citrus peels and apple pomace, and can be classified into high methoxyl pectin (HM-pectin) with DE (degree of esterification) > 50% and low methoxyl pectin (LM-pectin) with DE < 50% (Kjoniksen, Hiorth, & Nystrom, 2005; Strom et al., 2007). Both forms are capable of forming physical gels. LM-pectin can form gels at acid pHs or in the presence of divalent ions such as Ca (Capel, Nicolai, Durand, Boulenguer, & Langendorff, 2006; Gilsenan, Richardson, & Morris, 2000; Lootens et al., 2003), whereas HM-pectin forms gels in the presence of more than 55% sugar or a similar co-solute at pH <3.5 (Lofgren, Guillotin, Evenbratt, Schols, & Hermansson, 2005). For LM-pectin, hydrogen bonds and electrostatic interactions play a prominent role in the gelation mechanism (Kjoniksen et al., 2005). Hydrophobic interactions also contribute to the gelation of HM-pectin (Tho, Kjoniksen, Nystrom, & Roots, 2003). The strength of these interactions is influenced by both intrinsic (molecular weight, distribution of methyl esters, side chains, DE) and extrinsic factors (pH, ionic strength, Ca concentration, and temperature) (Capel, Nicolai, & Durand, 2005; Cardoso, Coimbra, & da Silva, 2003; Fraeye et al., 2009; Kjoniksen, Hiorth, & Nystrom, 2004; Lootens et al., 2003; Strom et al., 2007). Among these, solution pH is the most important factor affecting the gelation of LM-pectin. The electrostatic attractions are strongest when the pectin is almost fully charged at pH >4.5. Hence gels can be easily formed in the presence of Ca at high pHs (Capel et al., 2006). Ca ions enter into cavities provided by the pairing of the participating polygalacturonate sequences which adopt a two-fold zigzag conformation (Grant, Morris, Rees, Smith, & Thom, 1973). Recently, some researchers proposed that the binding process can be divided into two steps: monocomplexation and dimerisation (Dobies, Kusmia, & Jurga, 2005; Fang et al., 2008). The charge density of LM-pectin chain decreases with decreasing solution pH, which leads to a decrease in the sensitivity of pectin to Ca. At pH values lower than 2.0 the electrostatic interactions become negligible due to almost full protonation of charged groups (Capel et al., 2006), and as a result pectin chain becomes insensitive to Ca. However, the reduction in pH below 3.5 allows more carboxyl groups to act as hydrogen-bond donors and thus favours formation of hydrogen bonding-induced gels by dimerisation of three-fold helices (Gilsenan et al., 2000).

---

* Corresponding author. Tel.: +44 1978 29 3321; fax: +44 1978 293370.
E-mail address: s.alassaf@glyndwr.ac.uk (S. Al-Assaf).

0144-8617/$ – see front matter © 2012 Elsevier Ltd. All rights reserved.
http://dx.doi.org/10.1016/j.carbpol.2012.09.100

Aggregation/association in LM-pectin has long been recognised (Berth, Dautzenberg, & Hartmann, 1994). Recently, this subject has been studied to determine the influencing factors (especially intrinsic factors) (Cardoso et al., 2003; Kjoniksen et al., 2004, 2005; Kjoniksen, Hiorth, Roots, & Nystrom, 2003), and recently reviewed (Fraeye, Duvetter, Doungla, Van Loey, & Hendrickx, 2012). Nevertheless, the aggregation at various concentrations has not been fully characterised and for this reason we have systemically investigated the key roles of pH and intrinsic calcium present in commercial LM-pectin samples.

2. Material and methods

2.1. Materials

Fourteen commercial pectin samples were provided by different supplier companies. The samples were labelled as S1, S2, and S3 and so on. Degree of esterification (DE) and degree of amidation (DA) of these samples provided by the manufacturers are listed in Table 1. The test materials have various DEs ranging from 9.6% to 42.2% and DAs ranging from 0% to 25.7%. Among these samples, S3, S5 and S11–S14 were non-amidated.

2.2. Methods

2.2.1. Preparation of LM-pectin solutions

LM-pectin solutions were prepared by dispersing a weighted amount of pectin (based on solid content) into the appropriate solvent (distilled water, 0.2 M $NaNO_3$, 1 m $CaCl_2$, 1 mM Na_2EDTA, with varying concentrations of urea or mixed solutions of urea and $NaNO_3$), and left on a roller mixer for two days to fully hydrate. The intrinsic pHs for 5% aqueous pectin solutions of all samples were determined using an Orion 4 Star multifunctional pH metre (Thermo Electron Corporation, USA) at 25 °C.

2.2.2. Solubility

The solubility was determined according to the following method. A glass fibre filter paper (Fisherbrand MF 200) was weighed (m_1) after heating for 1 h at 105 °C followed by cooling down in a desiccator. 0.1 g (m_2) of sample was dissolved in 20 g of distilled water and left on a roller mixer to fully hydrate at room temperature overnight. Then the solution was filtered with the fibre filter under vacuum. The filter paper was weighted (m_3) again after drying at 105 °C for 1 h following by cooling in a desiccator. The solubility was determined by the following equation:

$$\%\,\text{solubility} = 100 \times \left(1 - \frac{(m_3 - m_1)}{m_2}\right) \quad (1)$$

2.2.3. GPC-MALLS

The molecular parameters of LM-pectin samples were determined using GPC-MALLS. The system mainly consists of a DAWN-DSP multi-angle light scattering photometer (Wyatt Technology, Santa Barbara, CA, USA) equipped with a He–Ne laser at the wavelength of 633 nm, a differential refractometer (RI 2000, Schambek, Germany) and an ultraviolet detector (Shimadzu SPD-6A, UK). 100 µL of 0.1 wt% LM-pectin solution was passed through a set of two columns SB-803HQ & SB-806HQ (8 mm × 300 mm) (Shodex OHpak, Japan – exclusion limits 1×10^5 and 2×10^7 g/mol) at a flow rate of 0.45 mL/min with 0.2 M $NaNO_3$ as the eluent. The eluent was passed through a degasser (ERC-3215α, ERC Inc., Japan) before being pumped into the GPC system using a constametric 3200 MS pump (Thermo Separation Products, USA). All samples were filtered through a 0.45 µm nylon filter prior to injection to the GPC system. A dn/dc value of 0.146 mL/g for LM-pectin reported previously (Cameron, Luzio, Goodner, & Williams, 2008; Fishman, Chau, Hoagland, & Ayyad, 1999) was taken for the determination of M_w.

2.2.4. Atomic adsorption spectrum

A flame atomic absorption spectrometer AANLYST 100 (Perkin Elmer, USA) furnished with a calcium hollow cathode lamp (422.7 nm) was employed to determine intrinsic Ca contents in the pectin samples according to the following method. Pectin solutions were prepared first by dispersing the ashes of 1 g of pectin samples into 250 mL of deionised water. The ashes were obtained by heating at 500 °C in a muffle furnace for 10 h after hydrolysis with concentrated H_2SO_4 at 150 °C for 1 h. Then the absorbance for every pectin solution was measured and was used to determine intrinsic Ca concentration in the LM-pectin solution by reference to a calibration curve of Ca concentration against absorbance. The calibration curve was constructed prior to the measurements through determining absorbance values of various known concentrations of $CaCl_2$ solutions (1, 2, 4 and 5 ppm). Finally, intrinsic Ca concentrations were converted to intrinsic Ca contents in the solid samples according to the following equation.

$$C\ (\text{ppm}) = \frac{(aA + b)\rho V}{m} \quad (2)$$

where a and b are the slope and intercept obtained from the calibration curve respectively, A is the atomic absorbance of pectin solution, ρ is the solution density taken as 1 g/mL, V is the solution volume (mL) and m is pectin mass (g) in the solution.

2.2.5. Intrinsic viscosity

Intrinsic viscosity measurements were performed using a calibrated Ubbelohde capillary viscometer (Cannon Ubbelohde Semi-Micro Calib 75) in a thermostated water bath at 25 ± 0.1 °C. Pectin solution (2 mL of 2.5 mg/mL) was introduced into the viscometer and followed by in situ dilution by additions of 0.4, 0.6, 1, 2, 4 and 5 mL solvent (0.2 M $NaNO_3$). The efflux times at different concentrations were determined in triplicate, and the average was taken. The efflux time of the solvent was also measured. The intrinsic viscosity was determined by a double extrapolation procedure according to Huggins and Kraemer equations (Morris et al., 2008):

$$\frac{\eta_{sp}}{c} = [\eta] + d_{\text{Huggins}}c = [\eta] + k'[\eta]^2 c\,(\text{Huggins}) \quad (3)$$

$$\frac{\ln(\eta_r)}{c} = [\eta] + d_{\text{Kraemer}}c = [\eta] + k''[\eta]^2 c\,(\text{Kraemer}) \quad (4)$$

where η_r is relative viscosity, η_{sp} is specific viscosity, c is polymer concentration (mg/dL), k' is Huggins constant, k'' is Kraemer constant, and d_{Huggins} and d_{Kraemer} are slopes of Huggins and Kraemer plots respectively. η_r is defined as:

$$\eta_r = \frac{\eta}{\eta_s} \quad (5)$$

and η_{sp} is defined as:

$$\eta_{sp} = \frac{\eta - \eta_s}{\eta_s} = \eta_r - 1 \quad (6)$$

where η and η_s are viscosities of polymer solution and solvent respectively. In dilute solution, the relative viscosity of a polymer solution is equal to the ratio of the efflux time t required for a specified volume of a polymer solution to flow through a capillary tube to the corresponding efflux time t_s for the solvent:

$$\eta_r = \frac{\eta}{\eta_s} = \frac{t}{t_s} \quad (7)$$

Table 1
Molecular parameters for pectin samples used in this study.

Sample	DE (%)	DA (%)	M_w (kDa)	M_w/M_n	pH	Ca content (ppm)	Solubility	$\eta_{0.1\ s^{-1}}$ (Pa s)
S1	30.1	19.8	183	3.63	4.14	988	96.6	5.0
S2	24.6	25.1	182	3.46	4.03	1388	96.6	17
S3	42.2	0	160	6.69	2.56	1062	85.8	65
S4	21.6	23.2	131	9.89	4.24	1210	96.8	1.0
S5	35.7	0	125	7.61	2.82	759	83.3	188
S6	29.9	18.6	178	3.27	4.20	655	97.1	4.4
S7	33.1	16.4	167	3.21	4.17	825	97.4	3.8
S8	37.8	12.2	290	5.85	4.21	299	95.2	3.8
S9	26.1	20.3	141	2.57	4.06	269	96.9	1.2
S10	29.9	25.7	134	7.56	4.26	1343	94.9	136
S11	34.9	0	153	5.07	3.50	847	93.4	19
S12	9.6	0	113	6.53	3.97	1299	82.2	0.3
S13	11.4	0	117	6.47	4.20	47	12.1	0.1
S14	24.7	0	153	9.62	3.89	47	77.4	3.3

Huggins and Kraemer constants can be obtained with following equations.

$$k' = \frac{d_{\text{Huggins}}}{[\eta]^2} \tag{8}$$

$$k'' = \frac{d_{\text{Kraemer}}}{[\eta]^2} \tag{9}$$

Additional measurement, to further confirm the role of hydrogen bonding, was also carried for S5 solution in the presence of 0.2 M $NaNO_3$ and 3 M urea.

2.2.6. Rheology

Steady shear rheological measurements were performed using AR-550 rheometer (TA Instruments, USA) fitted with a cone-and-plate geometry (60 mm diameter, 2.02° cone angle, and 58 μm gap) at room temperature. A thin layer of low-viscosity silicone oil (poly(dimethysiloxane), Sigma–Aldrich, USA) was applied around the cone to prevent solvent evaporation. Shear rate was increased from 0.05 to 500 s^{-1} (up curve), and then decreased from 500 to 0.05 s^{-1} (down curve). The zero-shear rate viscosity for different concentrations of pectin solutions was obtained by fitting the data with *Cross* model (Phillips & Williams, 2000):

$$\eta = \eta_\infty + \frac{\eta_0 - \eta_\infty}{1 + (\lambda \dot{r})^n}\ (\textit{Cross}\ \text{model}) \tag{10}$$

where $\dot{r}$ is shear rate, η_∞ is the infinite shear viscosity, η_0 is the zero-shear viscosity, λ is a shear-dependent constant denoting the onset of shear thinning, and n is an exponent quantifying the degree of shear thinning which has a value of 0 for a Newtonian solution and increases to 1 with increased shear thinning.

2.2.7. Dynamic light scattering

The role of salt on aggregation was investigated using a Zetasizer 1000HS photon correlation spectrometer (Malvern Instruments, UK) equipped with a He–Ne laser (633 nm) at a measuring angle of 90°. All measurements were carried out at 25 ± 0.1 °C. 0.1 wt% pectin solutions in the presence of $NaNO_3$ (or mixture of urea and $NaNO_3$) for DLS measurements were prepared by mixing equal volumes of 0.2 wt% pectin solution and $NaNO_3$ solution (or a mixed solution of urea and $NaNO_3$) together after filtration through a 0.45 μm nylon filter. The mixed solution was left in the cell for 1 h prior to the measurements.

The normalised field correlation function was fitted by a coupling model for analysing the dynamic features of a constrained and interacting system elaborated by Ngai and Phillies (1996) as given below:

$$g_1(t) = e^{-(t/\tau_{sc})^\beta} \tag{11}$$

where τ_{sc} is the effective characteristic time, and β is the stretching exponent which is a measure of the width of the distribution of relaxation time. The mean relaxation time can be given by the following equation:

$$\tau_s = \frac{\tau_{sc}}{\beta}\Gamma\left(\frac{1}{\beta}\right) \tag{12}$$

where $\Gamma(1/\beta)$ is the gamma function. The mean relaxation time τ_s is associated with relaxation of individual polymers or clusters (Kjoniksen et al., 2004). The hydrodynamic radius R_h was determined by the Stokes–Einstein equation (Mekhloufi, Sanchez, Renard, Guillemin, & Hardy, 2005):

$$R_h = \frac{k_B T}{6\pi \eta_s D_0} \tag{13}$$

where η_s is the solvent viscosity, k_BT is the thermal energy and D_0 is diffusive coefficient. D_0 can be obtained by the following equation:

$$D_0 = \frac{1}{q^2 \tau_s} \tag{14}$$

where q is the scattering wave vector. Prior to measurements, a standard monodisperse sample with a diameter of 60 nm was used for calibration.

3. Results

3.1. Characterisation of LM-pectins

Table 1 gives details of the samples used. The samples have high polydispersity and M_w as reported previously (Anger & Berth, 1986; Capel et al., 2005; Lootens et al., 2003). The mass recovery (data not shown) obtained from the ratio of mass eluted from column to the mass injected is in agreement with the values determined by independent measurement of solubility given in Table 1. Some of the non-amidated samples (S12–S14) showed poor solubility and some hydrogel was also present in S3, S5 and S11. The pH values for most of the samples were ~4 with exception of S3, S5 and S11. The low pHs for these three samples may be due to the acid hydrolysis employed for the extraction procedure and subsequently results in acid-induced aggregation (Capel et al., 2006). The calcium content varied greatly. Five samples (S2, S3, S4 S10 and S12) contained more than 1000 ppm. It is evident that some suppliers employ an additional step during the extraction to remove the calcium as shown for samples S13 and 14 and to a lesser extent in S8 and S9. The calcium content for other samples was in the range of 655–988 ppm. The intrinsic Ca concentrations in some samples was greater than 1 mM when the concentration reaches 5 wt%, which is sufficient to induce gelation according to some studies (Dobies et al., 2005; Narayanan, Deotare, Bandyopadhyay, & Sood, 2002).

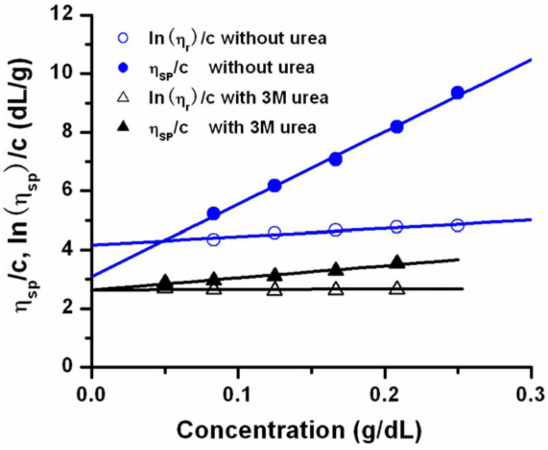

Fig. 1. Determination of intrinsic viscosity for S5 solutions with and without 3 M urea in the presence of 0.2 M $NaNO_3$.

3.2. Intrinsic viscosity

Intrinsic viscosity measurements were performed on all samples except S12, S13 and S14 due to the low solubility as noted above. Huggins and Kraemer plots for most of the samples intersect at zero concentration with the exception of S3, S5 and S11 as shown in Fig. 1 for S5. For these three samples, the intercept of Huggins plot at zero concentration was taken as intrinsic viscosity. For other samples, the average values of the intercepts of Huggins and Kremer plots at zero concentration were taken as intrinsic viscosity. The values of intrinsic viscosity together with Huggins and Kraemer constants (k', k'') are shown in Table 2. It can be seen that k' values are around 0.5, and $k' - k''$ are between 0.3 and 0.5 for the majority of the samples. However, for S3, S5 and S11, their Huggins constants are greater than 1, and $k' - k''$ departs substantially from 0.5, which indicate the presence of aggregates (Lewandowska, Staszewska, & Bohdaneck, 2001; Ma & Pawlik, 2007; Wang, Sun, & Wang, 2001). Note that all the samples giving Huggins constants greater than 1 have no amide groups.

The pH values of the samples with Huggins constant ~0.5 are higher than 3.5 where only Ca-induced aggregation may occur (Capel et al., 2006; Gilsenan et al., 2000; Lootens et al., 2003). Narayanan et al. (2002) investigated Ca-induced aggregation by dynamic light scattering and reported that at least 0.5 mM $CaCl_2$ was required for this to occur even in the presence of 0.1 M NaCl. The absence of aggregate in the dilute solutions can be attributed to low concentrations of intrinsic Ca present (smaller than 0.1 mM in 2.5 mg/mL solutions). The pH values of samples which give Huggins constant > 1 (S3, S5 and S11) are below 3.5. Low pHs favour the aggregation stabilised by hydrogen bonding (Gilsenan et al., 2000). Urea, a hydrogen bonding breaking agent which can inhibit the formation of hydrogen bonding by disrupting clusters of water molecules (Citri, Garber, & Sela, 1960; Sun & King, 1996), was added to the solvent to find if the high Huggins constants are exclusively due to aggregates stabilised by hydrogen bonding. The addition of urea to the solvent did not change the solution pH. Fig. 1 also shows intrinsic viscosity data for S5 in the presence of 3 M urea. In the presence of urea, Huggins and Kraemer plots intersect at the zero concentration with Huggins constant reduced from 1.42 to 0.57. Aggregation in dilute S5 solution can therefore be attributed to hydrogen bonding.

Table 2
Intrinsic viscosity and Huggins parameters for all pectin samples.

Sample	[η] (dL/g)	k'	k''	$k' - k''$
S1	3.99	0.54	0.10	0.44
S2	4.98	0.54	0.09	0.45
S3	3.86	1.27	−0.16	1.43
S4	2.89	0.54	0.07	0.47
S5	4.04	1.76	−0.26	2.02
S6	4.11	0.53	0.09	0.44
S7	3.96	0.57	0.07	0.50
S8	4.26	0.50	0.11	0.39
S9	3.73	0.45	0.11	0.34
S10	3.05	0.44	0.13	0.31
S11	3.15	6.09	−2.73	8.82

3.3. Rheology

Steady shear rheology measurements for 5 wt% aqueous solutions of all pectin samples were performed. The shear flow viscosity values at 0.1 s^{-1}, from the up curves, are shown in Table 1 and show no direct correlation with the intrinsic parameters (DE, DA and M_w). Extrinsic factors (pH, Ca content) and inter- and intramolecular distribution of the nonmethoxylated GalA residues could be responsible (Fraeye et al., 2009). The flow properties of all samples can be classified into three types (A, B and C). S3, S5 and S11 belong to type A. S1, S6 and S7 belong to type B. Other samples belong to type C. Fig. 2 shows the shear viscosity profile of selected samples. Samples S5 and S7 represent types A and B respectively, whereas both S8 and S9 represent type C. Type A exhibits strong shear thinning behaviour and type C exhibits a Newtonian plateau at low shear rates followed by shear thinning at high shear rates. Type B exhibits shear thinning at low shear rates, a Newtonian plateau at intermediate shear rates (0.5–10 s^{-1}) and again shear thinning at high shear rates. A viscosity difference between the up and down curves is evident in types B and C but not in type A. Shear thinning or thixotropic behaviour is often regarded as an indication of aggregation (Kjoniksen et al., 2005; Li et al., 2009). Thus aggregates could be present in types A and B aqueous solutions and to a lesser extent type C solutions.

The type A profile has been observed in aqueous LM-pectin solutions at pH values lower than 3.5 (Kjoniksen et al., 2005, 2003; Strom et al., 2007). Strom et al. (2007) compared viscosities as a function of shear rate for 1.5 wt% LM-pectin solutions at pHs 3.0 and 5.0. At pH 5.0 there was little shear rate-dependence whereas strong shear thinning region appeared as the pH decreased to 3.0. These workers proposed that the shear thinning was caused by the progressive breakdown of hydrogen bonding-stabilised aggregates. The rheological behaviour of type C is often found in aqueous solutions of hydrocolloids. The Newtonian plateau at low shear rates and the shear thinning at high shear rates can be attributed to molecular entanglement and molecular disentanglement respectively. There is less information about type B and we consider the shear thinning at low shear rates could be due to the breakdown of weak aggregates, followed by molecular disentanglement at high shear rates.

Fig. 3 shows the double logarithmic plot of zero-shear viscosity versus concentration of S5, S7, S8 and S9 with a corresponding slope of 7.5, 4.0, 3.8 and 3.3 in concentrated region respectively. The slope in the concentrated region of the double logarithmic plot of zero-shear viscosity versus concentration was often regarded as an indication of aggregation in polymer solution. For random coil polysaccharides which have no aggregates, the specific viscosity varies as $c^{3.3}$ in the concentrated region (Morris, Cutler, Ross-Murphy, Rees, & Price, 1981). However, higher values have been taken as evidence for hyperentanglement (Arvidson, Rinehart, & Gadala-Maria, 2006; Doyle, Lyons, & Morris, 2009). The highest slope for S5 with acidic pH could also be due to the aggregation stabilised by hydrogen bonding while the low slope for S9 implies the absence of aggregates. For S7 and S8, the deviation from the slope of 3.3 can be largely explained by the intrinsic Ca present

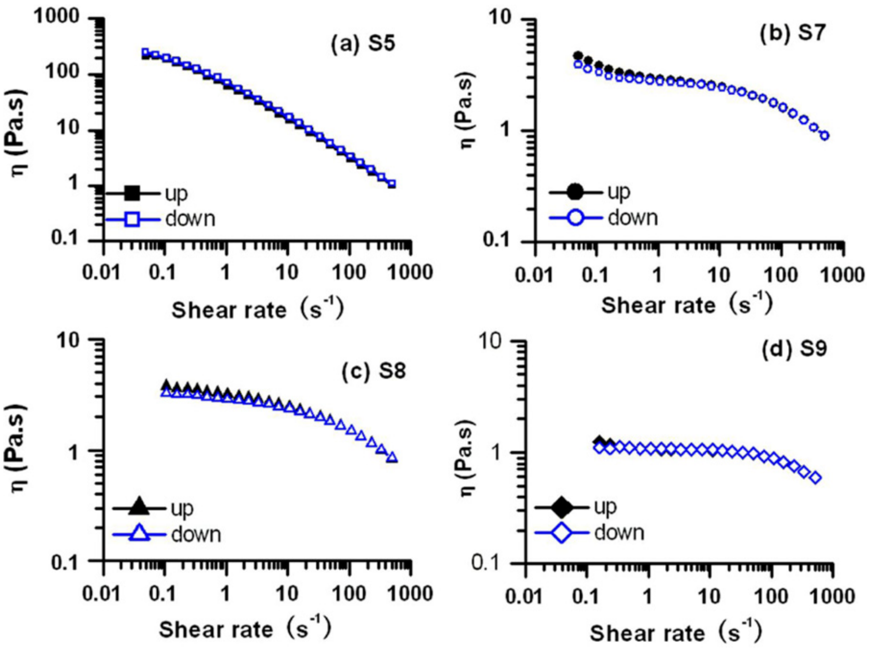

Fig. 2. Shear flow viscosity as a function of shear rate for 5 wt% aqueous solutions of (a) S5 (type A), (b) S7 (type B), (c) S8 (type C) and (d) S9 (type C).

since the pHs for 5% solutions of these two samples only allow Ca-induced aggregation. Unlike the method reported in previous studies (Morris, Cutler, et al., 1981), the concentration dependence of viscosity was measured in the absence of salt since we consider that the counterions present in the concentrated solution could screen intramolecular electrostatic repulsion effectively.

3.3.1. Effect of urea

Fig. 4 shows the effect of urea on the shear flow viscosity as a function of shear rate for 5 wt% S5. Urea significantly decreases the solution viscosity without a change in pH, indicating that hydrogen bonds play a leading role in the aggregation. We also investigated the effect of pH on the shear flow viscosity. Upon changing the solution pH from 2.8 to 3.5, the viscosity decreased dramatically (see Fig. 5), which shows that hydrogen bonding-induced aggregates only exist at pH values lower than 3.5 as reported previously (Capel et al., 2006; Gilsenan et al., 2000).

The concentration-dependence of the viscosity of S5 in the presence of 3 M urea was also carried out. Adding 3 M urea reduced the concentration-dependence of the viscosity of S5 from 7.5 to 3.3 (see Fig. 6), indicating that the aggregates is exclusively stabilised by hydrogen bonding. In the absence of urea the plot of viscosity versus concentration can be divided into three regions: dilute, semi-dilute and concentrated solutions. However, in the presence of 3 M urea, the plot divides into two regions as observed for the random coil hydrocolloid solutions without aggregates (Morris, Cut, Ross-murphy, & Rees, 1981). Moreover, the viscosity difference between these plots appeared when the concentration is above the coil overlap concentration, indicating that the aggregates are stabilised by intermolecular hydrogen bonding as proposed previously (Kjoniksen et al., 2004).

3.3.2. The effect of $CaCl_2$ and Na_2EDTA

It is clear that for types B and C, Ca-induced aggregation is dominant at pHs higher than 3.5 (Capel et al., 2006). So, we firstly used $CaCl_2$ to examine the contribution of Ca to the rheological behaviour for types B and C. Fig. 7 shows the effect of adding 1 mM $CaCl_2$ on the rheological behaviour of LM-pectin solutions. For the type B sample S7, the shear thinning at low shear rates disappears and is replaced by shear thinning at all shear rates. For type C samples S8 and S9, the extent of shear thinning is also enhanced as well as the separation between the up and down curves confirming Ca induced aggregation in types B and C.

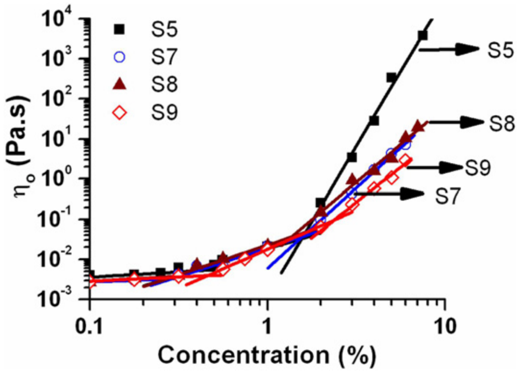

Fig. 3. Concentration dependence of viscosity for the aqueous solution of S5, S7, S8 and S9.

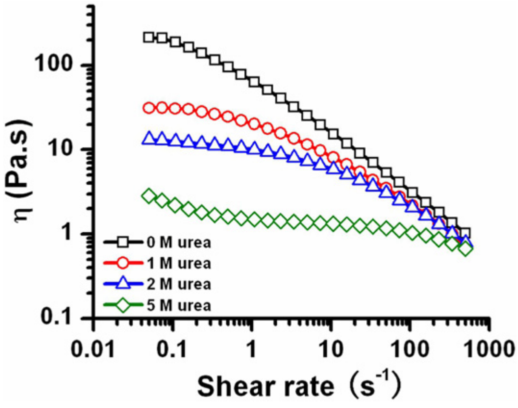

Fig. 4. Shear flow viscosity as a function of shear rate for 5 wt% aqueous S5 solution in the presence of various concentrations of urea.

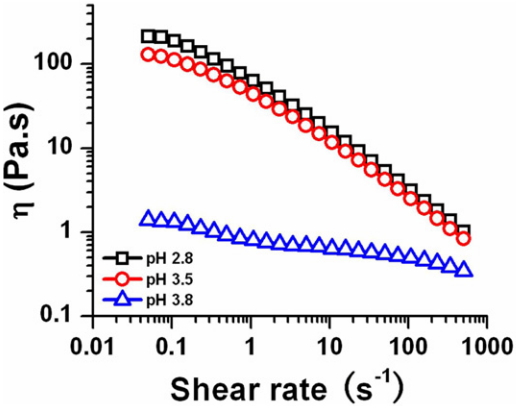

Fig. 5. Shear flow viscosity as a function of shear rate for 5 wt% aqueous S5 solution at various pH values.

For LM-pectin, aggregation occurs when the intrinsic Ca concentration reaches to a critical amount. However, only weak aggregates can be formed at low pH around pH 4 which are easily broken resulting in shear thinning. Thereafter, Ca-induced aggregates cannot be recovered immediately, probably because of the time needed for Ca ions to find suitable cavities formed by pairing of galacturonate sequences to accommodate the cations. This would account for the viscosity difference between the up and down curves which becomes larger with increasing concentrations of Ca ions due to the increased strength of aggregation. When the shear rate is higher than the onset of disentanglement, the two shear thinning regions separated by a Newtonian plateau are replaced by a single shear thinning region as seen in Fig. 7a.

Secondly, we have used a Ca-chelating agent Na_2EDTA to investigate the contribution of intrinsic Ca to the rheological behaviour. It is well established that the chelating ability of Na_2EDTA is negligible at pH 4.0 but significant at pH 7.0 (Liu, Qian, Shu, & Tong, 2003; Stokke et al., 2000). Thus the solution pH was adjusted to 7.0 prior to the addition of Na_2EDTA. Fig. 8 shows the shear flow viscosity as a function of shear rate for 5 wt% aqueous solutions of S7 and S8 in the absence and presence of Na_2EDTA at pH 7.0. Adjustment of pH only (i.e. absence of Na_2EDTA) resulted in decreasing the viscosity for both samples while the addition of Na_2EDTA further decreased the viscosity particularly for S7 (see Fig. 8). Pectin is almost fully charged above pH 4.5 (Capel et al., 2006) and thus can form strong Ca-induced aggregates. The aggregates are not easily broken down and/or can be recovered immediately, thus no viscosity difference between up and down curves is observed. The reduction in viscosity can be attributed to either dissociation of Ca-induced complexes due to $[EDTA]^{2-}$ complexing with Ca^{2+} or a decrease in polymer size due to Na^{+} screening the negative charges and consequently reducing charge repulsion. However, as seen in S8 (see Fig. 8b), the addition of a trace of salt (e.g. 1 mM) unlikely decrease the solution viscosity. Instead, partial screening of the electrostatic repulsion between adjacent chains could increase the probability of forming molecular association giving then an increase in solution viscosity as reported previously (Kjoniksen et al., 2005). Therefore the decrease in viscosity for S7 can only be attributed to the dissociation of Ca-induced aggregates following Ca ions complexing with $[EDTA]^{2-}$.

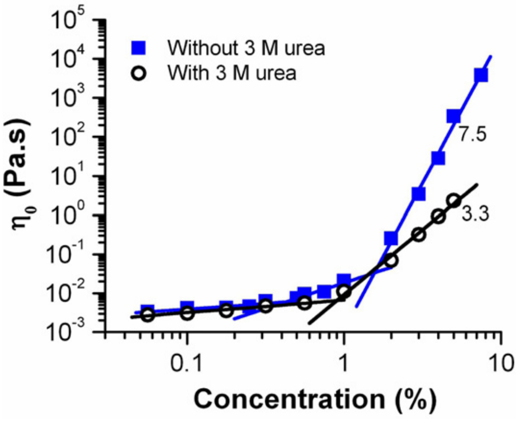

Fig. 6. Concentration dependence of viscosity for S5 with and without 3 M urea.

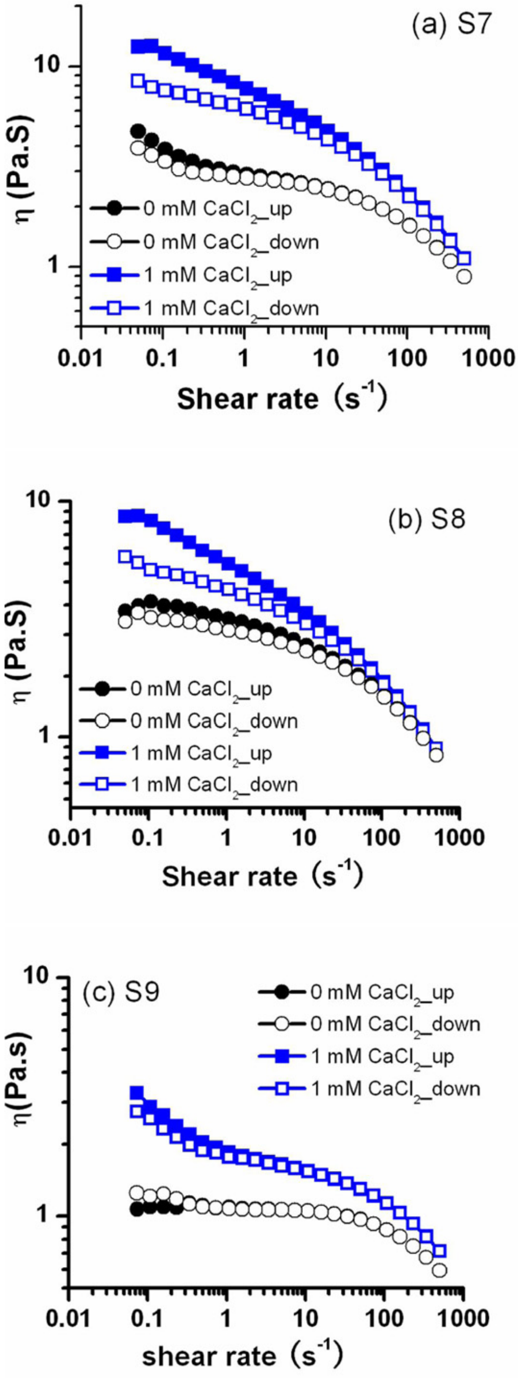

Fig. 7. Shear flow viscosity as a function of shear rate for (a) S7, (b) S8 and (c) S9 in the absence and presence of 1 mM $CaCl_2$.

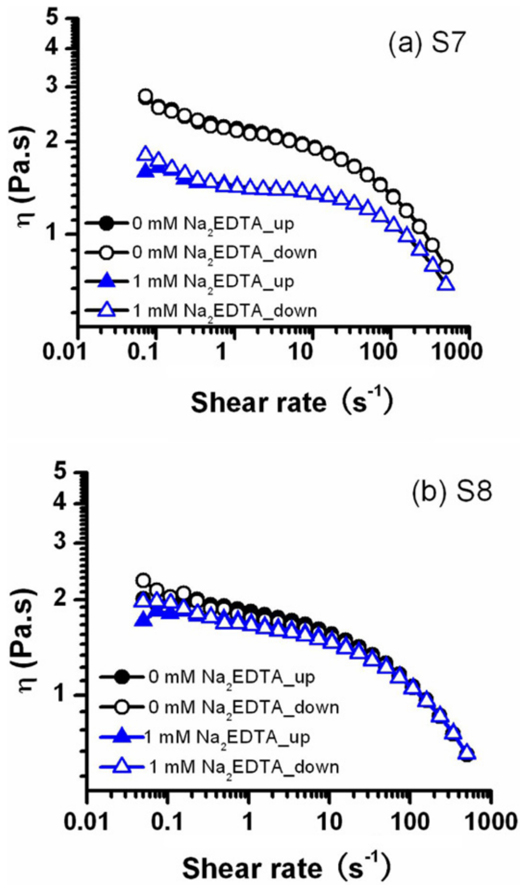

Fig. 8. Shear flow viscosity as a function of shear rate for 5 wt% (a) S7 and (b) S8 solutions in the absence and presence of 1 mM EDTA at pH 7.0.

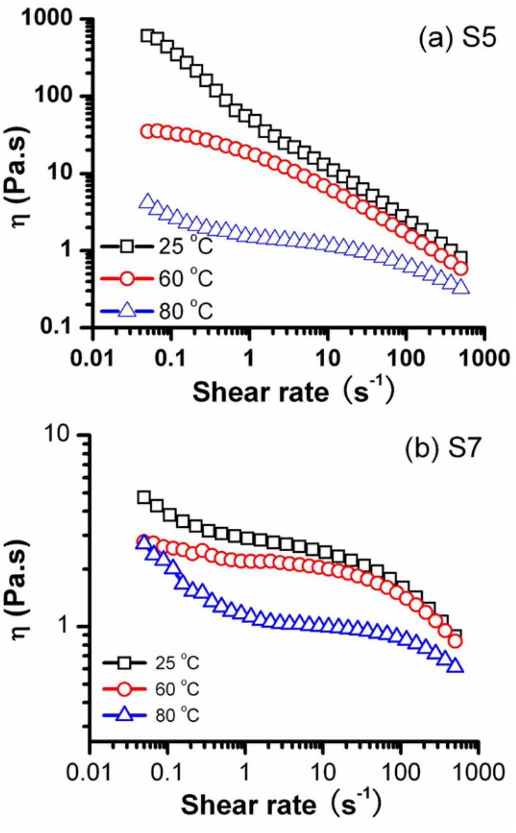

Fig. 9. Shear flow viscosity as a function of shear rate for aqueous solutions of (a) S5 and (b) S7, at room temperature before and after heating at 60 °C and 80 °C for 30 min.

3.3.3. The effect of temperature

Aqueous solutions of S5 and S7 were heated first at 60 °C and 80 °C for 30 min and subsequently allowed to cool down to room temperature. Fig. 9 gives the rheological behaviour of pectin solutions prepared at different temperatures (60 °C and 80 °C) compared to those prepared at room temperature. The increase of temperature reduced the viscosity for both samples but more so for S5, showing that preparing solution at higher temperatures favour Ca-induced aggregation other than the aggregation stabilised by hydrogen bonding. Recently, Kastner, Einhorn-Stoll, and Senge (2012) investigated structural transitions of LM-pectin during cooling. They reported that the structuring process started with ionic interactions via Ca-bridges at 60 °C followed by intermolecular hydrogen bonds below 25 °C. Therefore, Ca-induced aggregation occurs earlier than aggregation stabilised by hydrogen bonding during cooling. It is possible that Ca-induced aggregates formed at high temperature prevent the aggregation induced by hydrogen bonding at room temperature. It has been well established that at high temperatures the preferred conformation of LM-pectin is highly extended with local geometry close to the two-fold ordered structure, whereas it adopts compact three-fold structure at low temperatures (Gilsenan et al., 2000). Therefore, high temperature favours Ca-induced aggregation, while low temperature favour aggregation for hydrogen bonding. Moreover, the Ca binding energy at one binding site is a linear function of the length of non-esterified galacturonate sequences (Capel et al., 2005), so that two longer non-esterified galacturonate sequences will release more binding energy and form a more stable Ca-induced aggregate. Therefore, stronger Ca-induced aggregates can be formed when cooling from elevated temperatures as shown in Fig. 9. Meanwhile, the Ca-induced aggregates formed at high temperatures may prevent the formation of hydrogen bonding-induced aggregates during cooling, because it needs to overcome the electrostatic attraction between Ca ions and non-esterified galacturonate sequences before forming new hydrogen bonds.

However, two other possible reasons leading to the decrease of viscosity should be also mentioned. One possibility is that hydrophobic interactions could become stronger with increasing temperature and hence induce aggregation as observed in HM-pectin (Agoub, Giannouli, & Morris, 2009). However LM-pectin has weak hydrophobic interactions compared to HM-pectin. Kjoniksen et al. (2004, 2005), using dynamic light scattering, reported a decrease in LM-pectin chain size with increasing temperature and conclude that no hydrophobic aggregation occurs at high temperatures. The other one is that prolonged heating could induce depolymerisation due to β-elimination and/or acid hydrolysis (Fraeye et al., 2007), leading to a decrease in solution viscosity. LM-pectin solutions were often prepared at high temperatures so that they are fully hydrated (Capel et al., 2006; Cardoso et al., 2003; Fang et al., 2008). Here, it should be noted that preparing LM-pectin solutions at high temperatures could reduce their effectiveness as a thickener.

3.4. Dynamic light scattering

The effect of salt on aggregation was studied using dynamic light scattering (DLS). Fig. 10 gives the normalised field correlation function $g_1(t)$ at 90° for 0.1 wt% solutions of S5 and S7 in the presence of various concentrations of $NaNO_3$. As found in previous DLS studies of LM-pectin (Bulone, Martorana, Xiao, & San Biagio, 2002; Kjoniksen et al., 2004; Narayanan et al., 2002), there

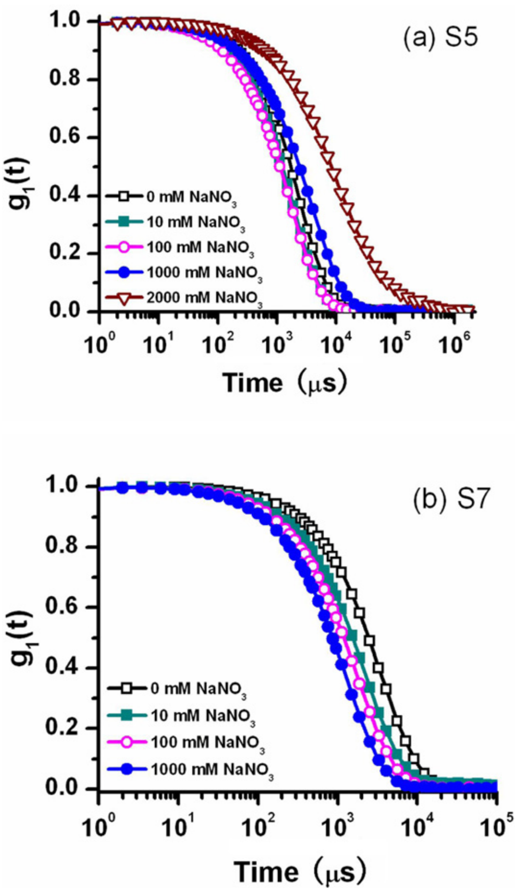

Fig. 10. Normalised field correlation functions for 0.1 wt% solutions of (a) S5 and (b) S7 in the presence of various $NaNO_3$ concentrations.

is a good fit between the coupling model and the normalised field correlation function. Fig. 11 shows the fitted values of relaxation times, stretching exponents and hydrodynamic radii. The relaxation time is in direct proportion to hydrodynamic radius, which can be understood readily by Eqs. (13) and (14). For S5, R_h decreases with the $NaNO_3$ concentration below 0.1 M but increases at concentrations > 0.1 M, which clearly shows that high salt concentration may induce aggregation in the dilute solutions of type A, as found with our intrinsic viscosity and rheology measurements. The aggregation stabilised by hydrogen bonding does not occur in dilute solution in the absence of salt (see Fig. 6) but is evident in the presence of 0.2 M $NaNO_3$ (see Fig. 1). R_h always decreases for S7 with increasing salt concentration due to salt screening of intramolecular electrostatic repulsion. It should be noted that β remained constant for S7, indicating that shrinkage of the polymer coil does not change the polydispersity. However, β decreases during salt induced-aggregation of S5, indicating that aggregation increases the polydispersity.

In order to identify the aggregation induced by high salt addition in S5 solution, urea was also employed. Fig. 12 shows the normalised field correlation function, and fitted values of relaxation time, R_h and stretching exponent for 0.1 wt% S5 solutions with various salt concentrations in the presence of 3 M urea. R_h decreases with increasing $NaNO_3$ concentration, suggesting that the aggregates induced by salt are stabilised by hydrogen bonds.

One possible explanation is that the appearance of aggregates in S5 solutions is caused by salting out, as proposed for HM-pectin by Yoo, Fishman, Savary, and Hotchkiss (2003) which is largely caused by hydrophobic interactions (Farinas, Scarpelini, Miranda, & Bertucci Neto, 2011). Such hydrophobic patches have a high degree

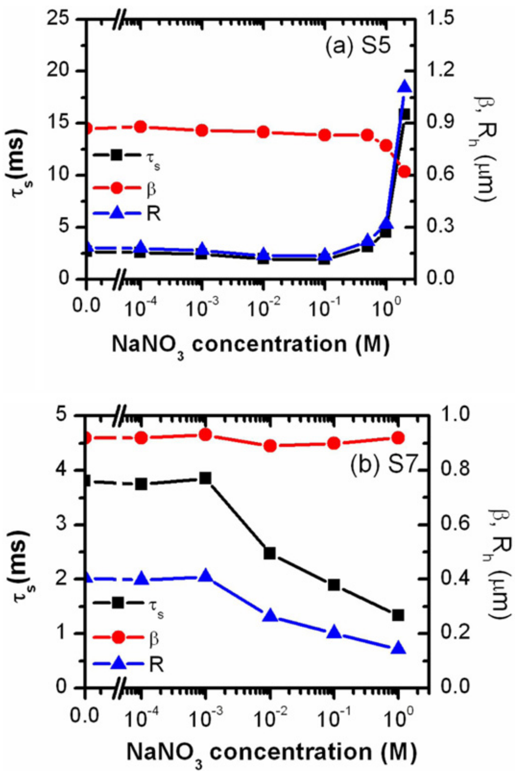

Fig. 11. Relaxation time, stretching exponent and hydrodynamic radius as a function of $NaNO_3$ concentration for (a) S5 and (b) S7.

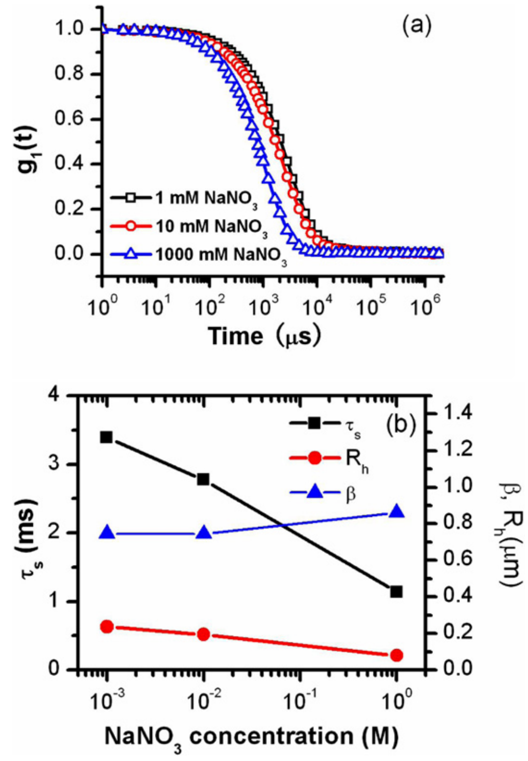

Fig. 12. (a) Normalised field correlation functions and (b) fitted relaxation times, stretching exponents and polymer size for 0.1 wt% S5 solutions with different salt concentrations in the presence of 3 M urea.

Table 3
Summary of main characteristics of different types of LM-pectins samples investigated in this study.

Type	A	B	C
Samples	S3, S5, S11	S1, S6, S7	S2, S4, S8, S9, S10, S12, S13, S14
Rheological behaviour	One strong shear Shearing	Two shear thinning and one Newtonian plateau	One shear thinning
Huggins constant	≥1	ca. 0.5	0.42–0.6
pH value in 5% (w/w) solution	<3.5	ca. 4.0	>3.5
Ca concentration in 5% (w/w) solution (mM)	0.95–1.3	~1	0.34–1.38
Slope in concentration dependence viscosity	High	ca. 4	3.38–3.75
Aggregation exists or not	Hydrogen bonding induced-aggregation	Ca-induced aggregation	Not determined

of ordering leading to a large decrease in entropy, and are thermodynamically unstable. The addition of salt will decrease the number of water molecules available for the hydrophobic patches by forming ion pairs with water molecules, and so causing hydrophobic aggregation and even precipitation. However, unlike HM-pectin, the hydrophobic interactions are not as strong as the hydrogen bonds in aqueous LM-pectin solutions (Kjoniksen et al., 2003; Lofgren et al., 2005). Furthermore, if the aggregation in S5 solution was caused by the salting out, it should also apply to S7 solution, however this is not the case. Therefore, rather than salting out we propose that aggregation is due to conformation transition induced by addition of salt. In the absence of salt, LM-pectin is highly extended due to strong intramolecular repulsions. Consequently the pectin chain is likely to still adopt a two-fold ordered structure, which does not favour the formation of the aggregates stabilised by hydrogen bonding because the aggregates form via dimerisation of three-fold helices (Gilsenan et al., 2000). Therefore, when the intramolecular repulsions are screened by high salt additions, the pectin chain preferentially adopts a compact three-fold structure, which favours the aggregation stabilised by hydrogen bonding.

4. Discussion

Molecular aggregation is a feature of aqueous LM-pectin solutions, and controls its functions as a gelling agent, stabiliser and thickener. Aggregation can be due to intrinsic factors, e.g. degree of esterification, degree of amidation, degree of blockiness, and extrinsic factors, e.g. pH and ionic strength. The influence of pectin fine structure has been well investigated (Fraeye et al., 2009, 2012; Strom et al., 2007), but there has not been a systematic study of the effect of extrinsic factors.

We find that the most important factors affecting aggregation are solution pH, which can adjust molecular conformation, the strength of hydrogen bonds and electrostatic interactions (see Table 3). At pH values higher than pH 4.5, the pectin chain is almost fully charged, resulting in strong electrostatic attractions between Ca ions and the pectin chains (Capel et al., 2006). The preferred conformation of LM-pectin at high pH is two-fold ordered structure (Gilsenan et al., 2000), so that high pH favours the formation of strong Ca-induced aggregates. However, when the pH is lower than 4.5, dissociation of pectin is partially suppressed leading to a decrease in the strength of electrostatic interactions. For some concentrated LM-pectin solutions, e.g. 5 wt%, the concentration of intrinsic calcium ions could be of the order of 1 mM, which is sufficient to induce aggregation. However, at low pHs around 4.0, LM-pectin only forms weak Ca-induced aggregates, which are easily broken down and do not recover immediately, resulting in shear thinning behaviour at low shear rates and a viscosity difference between up and down curves in type B or type C (see Fig. 2). At pH values below 3.5, the electrostatic interactions are significantly suppressed such that more carboxyl groups become hydrogen-bond donors and induce aggregation via a conformational transition from three-fold to two-fold helices (Gilsenan et al., 2000), then hydrogen bonding-induced aggregation readily occurs. Nevertheless, in dilute solution, the LM-pectin chain is likely to still have an extended conformation close to the two-fold helix structure because of the strong intramolecular electrostatic repulsion. Consequently, the aggregation stabilised by hydrogen bonding requires higher concentration than the overlap concentration. The hydrogen bonding-stabilised aggregation significantly increases solution viscosity causing strong shear thinning behaviour as observed for type A samples. After being broken down, the aggregates can recover immediately because the pectin readily forms hydrogen bonds with adjacent pectin segments, thus no viscosity difference is observed between the up and down curves (Fig. 2a).

Salt can also influence aggregation by changing the electrostatic interactions or molecular conformations. Reducing intermolecular electrostatic repulsive interactions allow aggregates to be formed more easily and so require less $CaCl_2$ as found by Narayanan et al. (2002). High NaCl addition can screen intramolecular repulsive interactions so that the LM-pectin chain is likely to adopt a compact three-fold structure, which enables aggregates stabilised by hydrogen bonding to be formed in dilute solution, as demonstrated by our intrinsic viscosity and dynamic light scattering results (Figs. 1 and 10).

Temperature is another important factor in the aggregation of LM-pectin. It adopts a compact three-fold structure at low temperatures and an extended two-fold conformation at higher temperatures (Cardoso et al., 2003; Gilsenan et al., 2000; Kjoniksen et al., 2004). Therefore, LM-pectin easily forms much stronger and ordered Ca-induced aggregates at higher temperatures. On the other hand, hydrogen bonding-induced aggregates are more easily formed at low temperatures.

5. Conclusions

Aggregation induced by hydrogen bonding or calcium are identified in aqueous solutions of commercial LM-pectins in this study. The formation of aggregates can be attributed to the intrinsic Ca and solution pH caused by their extraction procedure and subsequent processing. Additionally, the preparation temperature and ionic strength of pectin solution have also an important effect on the aggregation through adjusting intermolecular interactions and/or conformation. The presence of aggregates affects their solution properties and functionality significantly. Three types of rheological behaviour were identified. The roles of extrinsic factors have been identified which indicate how these can be used to optimise LM-pectin functionality.

Acknowledgements

The authors acknowledge the financial support from Phillips Hydrocolloids Research Ltd (U.K.) and the tuition fees waiver awarded to X. Li by Glyndwr University Wrexham.

References

Agoub, A. A., Giannouli, P., & Morris, E. R. (2009). Gelation of high methoxy pectin by acidification with D-glucono-delta-lactone (GDL) at room temperature. *Carbohydrate Polymers*, *75*(2), 269–281.

Anger, H., & Berth, G. (1986). Gel permeation chromatography and the Mark–Houwink relation for pectins with different degrees of esterification. *Carbohydrate Polymers*, *6*(3), 193–202.

Arvidson, S. A., Rinehart, B. T., & Gadala-Maria, F. (2006). Concentration regimes of solutions of levan polysaccharide from Bacillus sp. *Carbohydrate Polymers*, *65*(2), 144–149.

Berth, G., Dautzenberg, H., & Hartmann, J. (1994). Scattering light scattering technique appiled to pectin in dilute solution. 3. The tendency for association. *Carbohydrate Polymers*, *25*(3), 197–202.

Bulone, D., Martorana, V., Xiao, C. D., & San Biagio, P. L. (2002). Role of sucrose in pectin gelation: Static and dynamic light scattering experiments. *Macromolecules*, *35*(21), 8147–8151.

Cameron, R. G., Luzio, G. A., Goodner, K., & Williams, M. A. K. (2008). Demethylation of a model homogalacturonan with a salt-independent pectin methylesterase from citrus: I. Effect of pH on demethylated block size, block number and enzyme mode of action. *Carbohydrate Polymers*, *71*(2), 287–299.

Capel, F., Nicolai, T., & Durand, D. (2005). Influence of chain length and polymer concentration on the gelation of (amidated) low-methoxyl pectin induced by calcium. *Biomacromolecules*, *6*(6), 2954–2960.

Capel, F., Nicolai, T., Durand, D., Boulenguer, P., & Langendorff, V. (2006). Calcium and acid induced gelation of (amidated) low methoxyl pectin. *Food Hydrocolloids*, *20*(6), 901–907.

Cardoso, S. M., Coimbra, M. A., & da Silva, J. A. L. (2003). Temperature dependence of the formation and melting of pectin-Ca^{2+} networks: A rheological study. *Food Hydrocolloids*, *17*(6), 801–807.

Citri, N., Garber, N., & Sela, M. (1960). The effect of urea and guanidine hydrochloride on activity and optical rotation of penicillinase. *Jounal of Bioloqical Chemistry*, *235*(12), 235.

Dobies, M., Kusmia, S., & Jurga, S. (2005). H-1 NMR and rheological studies of the calcium induced gelation process in aqueous low methoxyl pectin solutions. *Acta Physica Polonica A*, *108*(1), 33–46.

Doyle, J. P., Lyons, G., & Morris, E. R. (2009). New proposals on “hyperentanglement” of galactomannans: Solution viscosity of fenugreek gum under neutral and alkaline conditions. *Food Hydrocolloids*, *23*(6), 1501–1510.

Fang, Y. P., Al-Assaf, S., Phillips, G. O., Nishinari, K., Funami, T., & Williams, P. A. (2008). Binding behavior of calcium to polyuronates: Comparison of pectin with alginate. *Carbohydrate Polymers*, *72*(2), 334–341.

Farinas, C. S., Scarpelini, L. M., Miranda, E. A., & Bertucci Neto, V. (2011). Evaluation of operational parameters on the precipitation of endoglucanase and xylanase produced by solid statc fermentation of aspergillus niger. *Brazilian Journal of Chemical Engineering*, *28*(1), 17–26.

Fishman, M. L., Chau, H. K., Hoagland, P., & Ayyad, K. (1999). Characterization of pectin, flash-extracted from orange albedo by microwave heating, under pressure. *Carbohydrate Research*, *323*(1–4), 126–138.

Fraeye, I., De Roeck, A., Duvetter, T., Verlent, I., Hendrickx, M., & Van Loey, A. (2007). Influence of pectin properties and processing conditions on thermal pectin degradation. *Food Chemistry*, *105*(2), 555–563.

Fraeye, I., Doungla, E., Duvetter, T., Moldenaers, P., Van Loey, A., & Hendrickx, M. (2009). Influence of intrinsic and extrinsic factors on rheology of pectin-calcium gels. *Food Hydrocolloids*, *23*(8), 2069–2077.

Fraeye, I., Duvetter, T., Doungla, E., Van Loey, A., & Hendrickx, M. (2012). Fine-tuning the properties of pectin-calcium gels by control of pectin fine structure, gel composition and environmental conditions. *Trends in Food Science & Technology*, *21*(5), 219–228.

Gilsenan, P. M., Richardson, R. K., & Morris, E. R. (2000). Thermally reversible acid-induced gelation of low-methoxy pectin. *Carbohydrate Polymers*, *41*(4), 339–349.

Grant, G. T., Morris, E. R., Rees, D. A., Smith, P. J. C., & Thom, D. (1973). Biological interactions between polysaccharides and divalent cations: Egg-box model. *FEBS Letters*, *32*(1), 195–198.

Kastner, H., Einhorn-Stoll, U., & Senge, B. (2012). Structure formation in sugar containing pectin gels – Influence of Ca(2+) on the gelation of low-methoxylated pectin at acidic pH. *Food Hydrocolloids*, *27*(1), 42–49.

Kjoniksen, A. L., Hiorth, M., & Nystrom, B. (2004). Temperature-induced association and gelation of aqueous solutions of pectin. A dynamic light scattering study. *European Polymer Journal*, *40*(11), 2427–2435.

Kjoniksen, A. L., Hiorth, M., & Nystrom, B. (2005). Association under shear flow in aqueous solutions of pectin. *European Polymer Journal*, *41*(4), 761–770.

Kjoniksen, A. L., Hiorth, M., Roots, J., & Nystrom, B. (2003). Shear-induced association and gelation of aqueous solutions of pectin. *Journal of Physical Chemistry B*, *107*(26), 6324–6328.

Lewandowska, K., Staszewska, D. U., & Bohdaneck, M. (2001). The Huggins viscosity coefficient of aqueous solution of poly(vinyl alcohol). *European Polymer Journal*, *37*(1), 25–32.

Li, X. B., Fang, Y. P., Al-Assaf, S., Phillips, G. O., Nishinari, K., & Zhang, H. B. (2009). Rheological study of gum arabic solutions: Interpretation based on molecular self-association. *Food Hydrocolloids*, *23*(8), 2394–2402.

Liu, X. X., Qian, L. Y., Shu, T., & Tong, Z. (2003). Rheology characterization of sol–gel transition in aqueous alginate solutions induced by calcium cations through in situ release. *Polymer*, *44*(2), 407–412.

Lofgren, C., Guillotin, S., Evenbratt, H., Schols, H., & Hermansson, A. M. (2005). Effects of calcium, pH, and blockiness on kinetic rheological behavior and microstructure of HM pectin gels. *Biomacromolecules*, *6*(2), 646–652.

Lootens, D., Capel, F., Durand, D., Nicolai, T., Boulenguer, P., & Langendorff, V. (2003). Influence of pH, Ca concentration, temperature and amidation on the gelation of low methoxyl pectin. *Food Hydrocolloids*, *17*(3), 237–244.

Ma, X., & Pawlik, M. (2007). Intrinsic viscosities and Huggins constants of guar gum in alkali metal chloride solutions. *Carbohydrate Polymers*, *70*(1), 15–24.

Mekhloufi, G., Sanchez, C., Renard, D., Guillemin, S., & Hardy, J. (2005). pH-induced structural transitions during complexation and coacervation of beta-lactoglobulin and acacia gum. *Langmuir*, *21*(1), 386–394.

Morris, E. R., Cut, A. N., Ross-murphy, S. B., & Rees, D. A. (1981). Concentration and shear rate dependence of viscosity in random coil polysacchaide solutions. *Carbohydrate Polymers*, *1*, 5–21.

Morris, E. R., Cutler, A. N., Ross-Murphy, S. B., Rees, D. A., & Price, J. (1981). Concentration and shear rate dependence of viscosity in random coil polysaccharide solutions. *Carbohydrate Polymers*, *1*(1), 5–21.

Morris, G. A., de al Torre, J. G., Ortega, A., Castile, J., Smith, A., & Harding, S. E. (2008). Molecular flexibility of citrus pectins by combined sedimentation and viscosity analysis. *Food Hydrocolloids*, *22*(8), 1435–1442.

Narayanan, J., Deotare, V. W., Bandyopadhyay, R., & Sood, A. K. (2002). Gelation of aqueous pectin solutions: A dynamic light scattering study. *Journal of Colloid and Interface Science*, *245*(2), 267–273.

Ngai, K. L., & Phillies, G. D. J. (1996). Coupling model analysis of polymer dynamics in solution: Probe diffusion and viscosity. *Journal of Chemical Physics*, *105*(18), 8385–8397.

Phillips, G. O., & Williams, P. A. (2000). *Handbook of hydrocolloids* (1st ed.). Cambridge: Woodhead Publishing. (Chapter 1).

Stokke, B. T., Draget, K. I., Smidsrod, O., Yuguchi, Y., Urakawa, H., & Kajiwara, K. (2000). Small-angle X-ray scattering and rheological characterization of alginate gels. 1. Ca-alginate gels. *Macromolecules*, *33*(5), 1853–1863.

Strom, A., Ribelles, P., Lundin, L., Norton, I., Morris, E. R., & Williams, M. A. K. (2007). Influence of pectin fine structure on the mechanical properties of calcium-pectin and acid-pectin gels. *Biomacromolecules*, *8*(9), 2668–2674.

Sun, T., & King, H. E. (1996). Aggregation behavior in the semidilute poly(N-vinyl-2-pyrrolidone)/water system. *Macromolecules*, *29*(9), 3175–3181.

Tho, I., Kjoniksen, A. L., Nystrom, B., & Roots, J. (2003). Characterization of association and gelation of pectin in methanol-water mixtures. *Biomacromolecules*, *4*(6), 1623–1629.

Wang, F., Sun, Z., & Wang, Y. J. (2001). Study of xanthan gum/waxy corn starch interaction in solution by viscometry. *Food Hydrocolloids*, *15*(4–6), 575–581.

Yoo, S. H., Fishman, M. L., Savary, B. J., & Hotchkiss, A. T. (2003). Monovalent salt-induced gelation of enzymatically deesterified pectin. *Journal of Agricultural and Food Chemistry*, *51*(25), 7410–7417.